STRUCTURAL AND TPS TRADE-OFF STUDIES AND DESIGN OPTIONS FOR THE HYPERSONIC TRANSPORT SYSTEM SPACELINER

Alexander Kopp [(1)], Nicole Garbers [(2)]

DLR Institute of Space Systems, Space Launcher Systems Analysis group (SART), Linzer Strasse 1, 28359 Bremen, Germany, Email: [(1)] alexander.kopp@dlr.de, [(2)] nicole.garbers@dlr.de

ABSTRACT

The SpaceLiner is a rocket propelled, hypersonic transport aircraft concept, with its launch being assisted by a separate booster stage.
This paper presents structural trade-off investigations for the SpaceLiner. Structural materials, structural concepts and member spacing will be compared, and the results discussed. The impact of minimum gauge thickness and TPS integration will be investigated as well. The analysis methodology will be described.
Furthermore, the integration of the passenger rescue stage into the vehicle structure will be addressed, with initial results being shown.

1. DESCRIPTION OF THE SPACELINER CONCEPT

Suborbital high speed transport is a technology that could significantly impact space transportation, since mass production of rocket propelled aircraft and their engines, as well as operating them on a routinely basis, promises reductions in the manufacturing and launching costs for space launchers. With this vision in mind, the SpaceLiner concept was developed in the Space Launcher Systems Analysis group (SART) of DLR in 2005. Since then, the original design has evolved into several successive configurations. The latest configuration 7-2 is shown in Fig. 1.

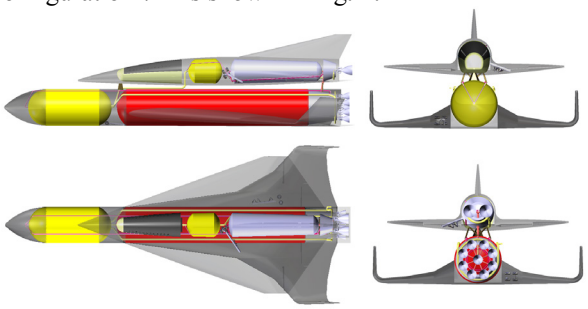

Figure 1. General configuration architecture of the SpaceLiner configuration 7-2

The SpaceLiner is a two stage, rocket propelled and vertical lift off passenger transport aircraft. The reference mission is to carry 50 passengers from Europe to Australia or vice versa within just 90 minutes. The SpaceLiner system is composed of a winged, passenger carrying main stage also denominated as orbiter, and a winged booster. Both stages are LOX/LH2 propelled, and fully reusable. After booster separation, the Orbiter continues the ascent with its own rocket engines until main engine cut-off at an altitude of around 75 km. Subsequently, the range flight is being performed in gliding mode, whereas Mach numbers of up to 24 are reached.
Obviously, the aero-thermodynamic loads are tremendous, leading to formidable requirements for the thermal protection system (TPS) and leaving little space for margins. Due to this, and the general problem of the comparatively low reliability of rocket propelled launch vehicles when compared to conventional passenger aircraft, it has been decided to accommodate the passengers in a separate crew rescue stage (CRS). The CRS is designed such that it can be separated at any point of the mission and transport the passengers back to ground safely.
In the past, the focus of the SpaceLiner design investigations was on aero-thermodynamic and mission optimization, as well as on propulsion system layout. Currently, the focus is shifting more to structural design and structure-TPS integration. Indeed, the vehicle is highly mass critical and very light-weight structures are mandatory in order to allow for the feasibility of the vehicle and its mission.
The booster stage is a comparatively conventional configuration, whereas the orbiter is a more complex design with much higher performance and safety requirements. Thus, the current structural investigations concentrate mainly on the orbiter stage.

2. STRUCTURAL ANALYSIS METHODOLOGY

In early flight vehicle design phases it is common practise to apply statistical/empirical methods in order to estimate the structural mass of a new concept. However, these methods are obviously of limited benefit if unique configurations are being investigated that have no representations in the statistical database. In these cases, it is reasonable to apply structural analysis methods already in early design phases.

2.1. HySAP – Hypersonic Vehicle Structural Analysis Program

For structural analyses of the SpaceLiner orbiter, the program HySAP (Hypersonic vehicle Structural Analysis Program) is being applied, which has been developed by DLR-SART. HySAP combines Fortran based pre-processor and sizing routines with the ANSYS-APDL environment. Fig. 2 displays the general program architecture. The pre-processor generates an APDL input file for ANSYS, which contains all commands for modelling, structural analysis, and post-

processing. After finishing the solution, the sizer is being called which performs structural sizing according to various strength and stability failure modes/design criteria. The adapted wall thicknesses are transferred back to ANSYS, and the computation is restarted. On this way, the structure is iteratively adapted in accordance with "fully stressed design" principles, until convergence has been reached. More detailed program descriptions have been published in [1] and [2].

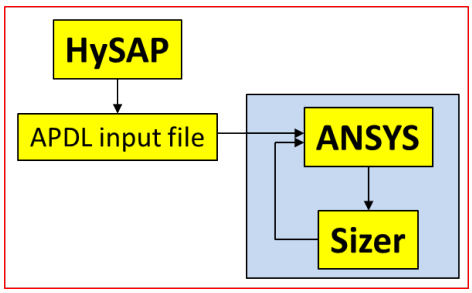

Figure 2. HySAP general program architecture

HySAP serves for rapid modelling and structural analysis of almost arbitrary vehicle configurations. It is usually applied for trade-off studies in order to allow for determining optimum structural designs, or even vehicle configurations. In the past is has been applied within the EC co-funded FP7 studies FAST20XX, LAPCAT-II, and ATLLAS-II.

2.2. HySAP – Geometry and Loads Modelling

HySAP receives geometry and loads inputs from other system analysis tools, whereas the modelling procedure is fully automated. An aerodynamic mesh is provided, which will be exploited to generate the external geometry in ANSYS. The aerodynamic mesh provides also the pressure distribution. A TPS thickness distribution over the vehicle surface can be provided as well. In this case, the local TPS thicknesses will be subtracted from the external surface, yielding an adapted structural geometry. Propellant tank geometries and loads will be provided by other tools as well, and modelled automatically. Sub-systems will be modelled as point masses, and attached to frames, ribs and spars via rigid and massless elements.
Structure materials, structure concepts, and the internal structure geometry (e.g. position of structural members) have to be specified, whereas an automated positioning procedure can be applied for the latter, if desired. Currently, unstiffened and stringer-stiffened skins as well as honeycomb sandwich concepts can be analysed. Additional concepts will be added in future modifications. Stringer stiffening and sandwich designs are modelled via multi-layer shell elements.

2.3. HySAP – Structural Analysis and Adaption

An arbitrary number of load cases can be processed by HySAP. The inertia relief capability of ANSYS will be exploited for free flight load cases.
After ANSYS has finished the solution, the relevant geometry and material data are sent to the Fortran sizer. This tool evaluates the structure against various strength and stability failure modes, using analytical methods. Thereby, each panel or each structural component will be analysed individually according to its local load environment. Wall thicknesses and other parameters such as stringer spacing and stringer or core heights will be adapted, and the new wall thicknesses and stiffener data sent back to ANSYS. Subsequently, ANSYS restarts the FE analysis with the adapted wall thicknesses. This procedure is repeated until convergence has been reached. Thereby, convergence is defined when the structural mass change between four successive iterations remains within a user defined percentage limit.

2.4. HySAP – Non-Optimum Mass Consideration

A method for consideration of non-optimum masses (NOM) has been developed and implemented recently in HySAP. In preliminary structural analysis of aerospace vehicles, usually the main structural members such as skin panels, ribs, spars, frames, stringers, etc. are being analysed and sized according to stress and stiffness/stability design criteria. However, the resulting structural mass does not represent the structural mass of a real flight vehicle since it does not consider NOM contributions. This may include various items such as joints, fasteners, attachments, bolts, welding, rivets, cut-outs, manufacturing tolerances, and others. NOM contributions have to be included in the structural mass budget; otherwise the structural mass would greatly be underestimated. This is even more the case for aircraft like vehicles, since they tend to have higher NOM fractions when compared to rocket launchers. It is obvious, that on a preliminary design stage empirical/statistical approaches are required in order to estimate the NOM contributions.
For hypersonic vehicles no statistical databases are available. Thus, for HySAP a new procedure for NOM consideration has been developed. Thereby, the non-optimum factors (NOF) are computed group-wise for wings, fuselages, tank cylinders/cones, and tank domes. The computed optimum structural mass will then be multiplied with the NOF to form the final mass.
The NOF approach developed here consist of two components: a basic factor NOF_{basic} that is dependent on the group structural mass (such as wing structure mass for example), and a structural concept dependent $NOF_{concept}$, which reflects the particular structural design (e.g. unstiffened, stringer stiffened, or sandwich). The final NOF is then computed by Eq. 1.

$$NOF_{final} = NOF_{basic} NOF_{concept} \quad (1)$$

The relationships for estimating NOF_{basic} have been derived from [3]-[6]. The concept dependent $NOF_{concept}$ on the other hand have been assembled with data from [7]-[10].

3. VEHICLE AND LOADS MODELLING

3.1. Structure Model of the SpaceLiner

For the current parametric studies a simplified geometry model of the SpaceLiner is being used. A more detailed model will be generated as soon as the structural configuration design has matured. Fig. 3 displays the current internal structure geometry. The forward pressure vessel represents the LOX tank, the aft one the LH2 tank. In this analysis, the tanks are completely connected with all neighbouring fuselage frames/bulkheads. Thus, the tanks support the fuselage with carrying the bending loads, thus yielding lower fuselage-, but higher tank weights.

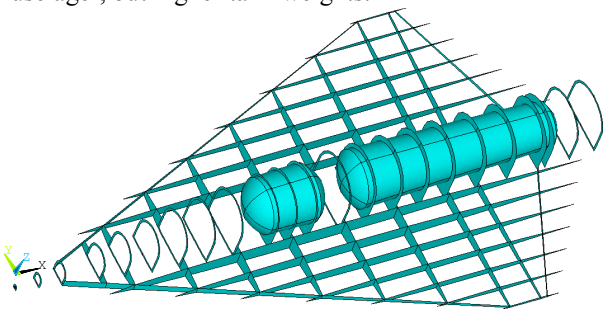

Figure 3. Simplified structure geometry model for the SpaceLiner orbiter

The fuselage utilizes stringer stiffened skins with frames/bulkheads made of honeycomb sandwich. The wing ribs, spars, and skins are completely designed as sandwich structures. The propellant tanks are stringer stiffened with unstiffened domes. The fin has been neglected in this analysis.

3.2. Loads and Assumptions

A total of 4 load cases have been considered. These are:

- LC1: Maximum axial acceleration during ascent; the orbiter is attached to the booster
- LC2: n_z = 2.5 g normal acceleration manoeuvre with wing flap deflection
- LC3: n_z = 2.5 g normal acceleration manoeuvre without wing flap deflection
- LC4: nz = -1.0 g normal acceleration manoeuvre with wing flap deflection

Tab. 1 summarizes the load case data. In the load cases 2-4 the inertia relief capability of ANSYS is applied. Thus, the given acceleration levels are only approximate since the actual accelerations depend on the vehicle weight, which is not exactly known before the analysis.
In LC1 the tanks are still partly filled. The high static pressures result from a propellant cross-feeding system where propellants from the booster are transferred to the orbiter tanks. In the analysis, the static pressures will be increased by the hydrostatic pressures that result from the acceleration levels. In the other load cases the tanks are empty. Residuals and reserves are neglected here.
The aerodynamic pressure distributions have been computed with an inclination based code for hypersonic aerothermodynamics. The angles of attack (AoA) have been adapted such that the desired n_z accelerations are obtained.
All considered subsystems including passenger cabin and payload sum up to a total mass of 88 t for the current configuration. They are located in fuselage and wings at the appropriate positions.

Table 1. Load case data

	LC1	LC2	LC3	LC4
Axial acceleration [g0]	2.4	≈ -0.5	≈ -0.9	≈ -0.4
Normal acceleration [g0]	0.1	≈ 2.5	≈ 2.5	≈ -1.0
Angle of attack [°]	0.2	15.5	18.0	-4.0
Ma [-]	3.8	8.6	8.6	8.6
Altitude [km]	35.2	38.2	38.2	38.2
Static pressure LOX [bar]	8.5	2.0	2.0	2.0
Static pressure LH2 [bar]	2.5	2.0	2.0	2.0
Propellant mass [t]	72.8	0.0	0.0	0.0

A safety factor of 1.5 has been applied to all strength and stability failure modes. A minimum gauge thickness of 0.25 mm has been considered initially, but will be adapted later (section 4.2).

3.3. Design of Thermal Protection System

A preliminary TPS has been designed, with the allowed structure temperature for the orbiter set to 530 K. Different surface temperature regions have been defined (Fig. 4). For each of these regions, a separate TPS thickness has been computed, whereas CMC, AETB, TABI, and AFRSI material systems are used.

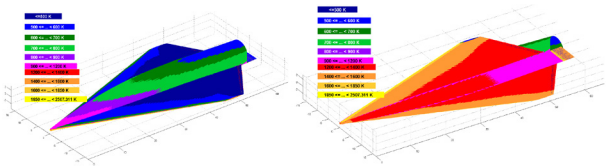

Figure 4. Definition of temperature regions

The TPS design yielded in TPS thicknesses of up to 34 cm. These thicknesses will be subtracted from the external mould line in order to form the structural geometry.
The allowed back-structure temperatures are too high for the application of aluminium, for instance. Therefore, separate TPS designs tailored to the particular structural material will be generated in future investigations. Previous preliminary investigations yielded a strong dependence of the TPS mass on the allowed structural temperatures (Tab. 2).

Table 2. Preliminary TPS mass estimations

Allowed structural temperature [K]	TPS mass [t]
400	34.2
480	28.7
530	25.6

4. STRUCTURAL DESIGN TRADE-OFFS

With the vehicle model and the applied loads as

described before, several parametric studies have been performed. These investigations are still ongoing, with intermediate results being presented here.

4.1. Structure Materials and TPS Integration

The selection of the structural materials obviously has a major impact on the vehicle mass. Materials with high specific strength and stiffness are required. For hypersonic vehicles, also the temperature resistance is of crucial importance.
In this study, only the metallic materials aluminium, titanium, and aluminium-lithium have been considered. Further studies will also include CFRP composites. Also temperature effects have been neglected, but will be addressed in future analysis. The applied material properties are listed in Tab. 3.

Table 3. Material data

Material	ρ [kg/m^3]	E [N/m^2]	σ_{yield} [N/m2]
Al	2.796	$7.24 \cdot 10^{10}$	$3.31 \cdot 10^{8}$
Ti	4.430	$1.138 \cdot 10^{11}$	$8.28 \cdot 10^{8}$
Al-Li	2.710	$7.60 \cdot 10^{10}$	$4.90 \cdot 10^{8}$

The TPS design as discussed in section 3.3 has been used. The integration of the TPS will yield a reduction of structural construction height, which in turn leads to higher bending stresses, and therefore higher structural masses. This effect has been considered for all three materials. The resulting structural masses are shown in Fig. 5. For each of the three materials, the structural mass without (left column), and with (right column) TPS consideration is presented. In the last two columns, a further calculation is shown for an aluminium structure, but in this case the stringer stiffened fuselage has been replaced by sandwich design.

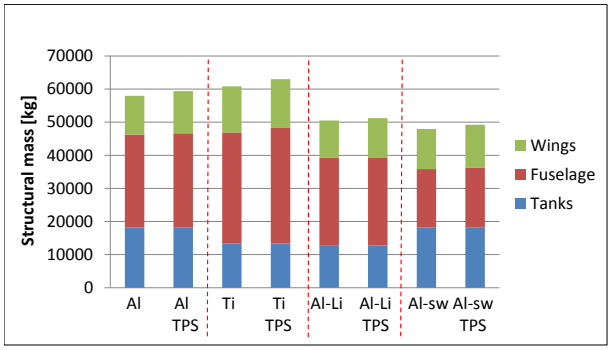

Figure 5. Computed structural masses without and with TPS consideration for different structure materials

In all four cases a mass increase can be assessed when a structure construction height reduction due to TPS integration is been considered. These are (from left to right) 2.4 %, 3.6 %, 1.4 %, and 2.7 %. Also, the lowest Eigen-frequencies reduce in the order of 0.5-1.0 Hz when TPS is considered. For the aluminium structure with stringer-stiffened fuselage for instance, the first Eigen-frequency (symmetrical wing bending mode) decreases from 4.5 to 3.85 Hz.
Furthermore, the large weight advantage of aluminium-lithium is evident. Finally, the change of the fuselage stringer-stiffening to sandwich design yields a major weight decrease. However, in this case also the lowest Eigen-frequencies decrease significantly. For example, the third Eigen-frequency (combined fuselage & wing bending) reduces from 7.6 to 6.2 Hz. It also has to be noted that the competitiveness of stringer stiffening greatly increases when reducing the frame spacing (section 4.3).
Titanium and aluminium-lithium structures yield low tanks weights compared to aluminium, thanks to their higher specific strength. Due to the high internal pressures, the tanks are to a large extent sized by strength, rather than stability.

4.2. Increase of Minimum Gauge Thickness

A large number of structural members are not sized by evaluation against failure modes. Instead, if the local loads are small, the member will be sized down to the minimum gauge thickness. Thus, the impact of increasing the minimum gauge thickness was evaluated. For this, the original gauge thickness of 0.25 mm was doubled to 0.5 mm. The results are shown in Fig. 6. In all cases the TPS integration was included.

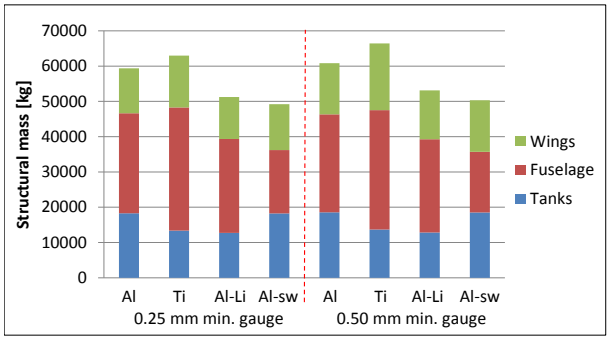

Figure 6. Impact of minimum gauge thickness increase from 0.25 mm (left) to 0.5 mm (right)

A structural mass increase between 2.2 and 5.5 % was found. Thereby, the mass increase is almost completely the result of higher wing masses. Indeed, for the wings alone, the mass increase is between 12.4 and 29.0 %.

4.3. Reduction of Frame Spacing

The fuselage frame spacing has a major impact on the fuselage mass. In particular, reducing the panel length between two frames will greatly reduce the skin and stringer buckling vulnerability, and thus yielding lower wall thicknesses and stringer dimensions.
The baseline structural model as shown in Fig. 3 has several fixed frame stations, for example at beginning and end of the tank cylinders, as well as at wing-spar/fuselage attachment positions. The space in between these fixed frame stations has been filled with additional frames by assuming an average spacing of 4.0 m. This average frame spacing has now being reduced stepwise down to 2.5 m. The results are shown in Fig. 7 (aluminium, 0.5 mm minimum thickness).

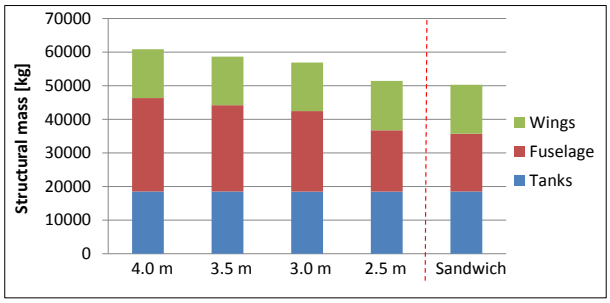

Figure 7. Impact of frame spacing reduction on structural mass (aluminium structure)

A significant fuselage mass decrease was found when reducing the frame spacing. In contrast to the results shown in Fig. 5, stinger stiffening of the fuselage is now competitive with sandwich design.

4.4. Evaluation of Applied Design Criteria

An evaluation of the design criteria provides valuable information for future optimizations. As one example, the aluminium structure with 0.5 mm minimum thickness will be discussed here.

The sandwich core thicknesses will be adapted in order to prevent global buckling. The final core thicknesses reach values of up to 57 mm. Fig. 8 shows the sandwich core thicknesses for the wing panels. The skin panels have in average higher thicknesses (left) compared to spars and ribs (right).

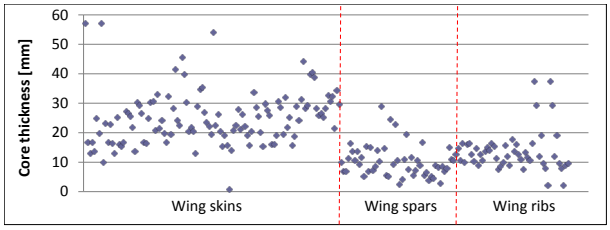

Figure 8. Wing sandwich core thicknesses

The majority of the wing sandwich face-sheets have been sized against von Mises stress or remain on the minimum gauge thickness. A total of 18 % of the panels were sized by face wrinkling. The fuselage frame sandwich structures instead were all sized against von Mises stress (face-sheets), and shear-crimping (core), respectively.

Fig. 9 shows the stringer heights for the fuselage. The maximum height has been limited to 150 mm in this investigation. The stringer pitch is connected to the stringer height via a simple relationship.

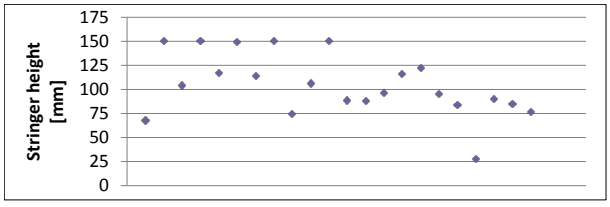

Figure 9. Fuselage section stringer heights

The fuselage stringers were mainly sized against local buckling, while the skins were partly sized by sheet buckling, and von Mises stress, respectively. The tanks skins on the other hand were almost completely sized against von Mises, while the stringer usually remained on minimum thickness.

4.5. Evaluation of NOM Factors

As outlined in section 2.4, the NOF for a structural group are a function of the specific structural concept, and the overall wing or fuselage structural mass. For the configuration discussed in section 4.4, the computed and applied NOF are listed in Tab. 4. It is obvious, that a large fraction of the vehicle structure mass is resulting from NOM contributions.

Table 4. Computed NOF

Group	Panel concept	NOF
Wing skins, spars, ribs	Sandwich	1.65
Fuselage skins	Stringer stiffened	1.31
Fuselage frames	Sandwich	1.56
Tank skins	Stringer stiffened	1.25
Tank domes	Unstiffened	1.59

5. RESCUE STAGE INTEGRATION

The integration of the CRS into the orbiter structure is a major design issue. A safe and fast separation has to be assured at every point of the mission, while simultaneously the CRS integration must not yield a significant increase in orbiter structural mass. This issue is subject of comprehensive ongoing system investigations. Thus, only preliminary results can be presented here. Fig. 10 shows two possible configurations. Concept A is the baseline configuration. The CRS is encapsulated in the vehicle structure, whereas the upper part of the CRS is also part of the orbiter structure. For concept B the whole vehicle nose forms the CRS. The advantages and disadvantages of both concepts have been analysed on a system level approach in [11], and are summarized in Tab. 5.

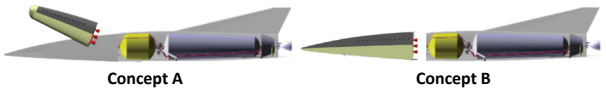

Figure 10. CRS integration/separation concepts [11]

Concept A	Concept B
+ Lower CRS mass	+ Simple integration
+ Impact protection	+ Faster separation
- Extra time for erection	+ Lower loads
- High AoA at separation	+ Higher L/D ratio
- Higher loads	+ low AoA at separation
- complex separat. procedure	- no impact protection
- double TPS and structure	- higher CRS mass
- weakening of orbiter structure	

Table 5. Advantages (+) and disadvantages (-) for CRS concepts A and B [11]

The less complex concept B offers numerous advantages. However, a major drawback is the missing impact protection. One important emergency case that could result in a CRS separation, is a damage of the orbiter TPS (e.g. due to impacts). In concept B however, a damage of the forward orbiter TPS is simultaneously also a damage of the CRS TPS. In that case, the CRS would be unable to assure a safe return of the passengers to the ground after separation.
On the other hand, one of the major drawbacks of concept A is the weakening of the orbiter structure due to the large cut-out. Preliminary studies have been launched using HySAP in order to investigate the mass penalty. Initial calculations indicated an increase of orbiter structural mass in the order of 15 %. Also the first Eigen-frequencies reduce and reveal modes that are directly associated with the cut-out (Fig. 11).

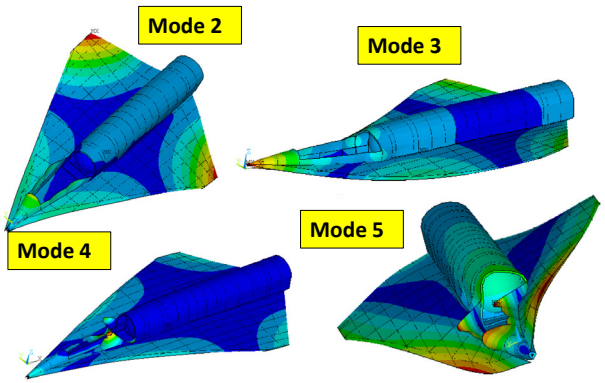

Figure 11. Eigen-modes 2-5

More results on the CRS integration and the impact on the vehicle structure will be presented in [12].

6. CONCLUSION AND OUTLOOK

Parametric trade-off studies are currently being performed for the SpaceLiner orbiter structure. Intermediate results have been presented here, and reveal a significant impact of the selection of minimum gauge thickness, as well as the TPS integration on the vehicle mass. The competitiveness of structural concepts and materials is depending on the particular structural geometry. Furthermore, initial results of the CRS integration studies have been shown.
In future works, the interaction of TPS and structure will be addressed in detail. In particular, different TPS will be designed for different structural materials and allowed structural temperature levels. The impact of increased temperatures on the structural material properties will be considered. Also, CFRP composites will be addressed as alternatives to metallic materials.
Finally, the CRS design and integration will be investigated in more detail. This will be done on a comprehensive system level.

7. REFERENCES

1. Kopp, A. (2012). Parametric Studies for the Pre-Design of Hypersonic Aerospace Vehicles. 12th European Conference on Spacecraft Structures, Materials, and Environmental Testing, Noordwijk, The Netherlands
2. Kopp, A., Garbers, N., Jarlas, R., Rabia, H. (2012). Parametric Structural Analysis for the SpaceLiner. 18th AIAA/3AF International Space Planes and Hypersonic Systems and Technologies Conference, Tours, France
3. Ardema, M. D., Chambers, M. C., Patron, A. P., Hahn, A. S., Miura, H., Moore, M. D. (1996). Analytical Fuselage and Wing Weight Estimation of Transport Aircraft, NASA-TM-110392
4. Reitz, G. R. (1967). The Derivation and Application of Nonoptimum Factors for Missiles and Spacecraft. 26nd SAWE Annual Conference, Boston, USA
5. Wu, K. C., Cerro, J. A. (2010). Hardware-Based Non-Optimum Factors for Launch Vehicle Structural Design. NSMMS - National Space and Missile Materials Symposium; Scottsdale, USA
6. Wu, K. C., Wallace, M. L., Cerro, J. A. (2013). Development of Non-Optimum Factors for Launch Vehicle Propellant Tank Bulkhead Weight Estimation. 51st AIAA Aerospace Sciences Meeting, Grapevine, USA
7. Plank, P. P., Sakata, I. F., Davis, G. W., Richie, C. C. (1970). Hypersonic Cruise Vehicle Wing Structure Evaluation. NASA-CR-1568
8. Plank, P. P., Sakata, I. F., Davis, G. W., Richie, C. C. (1970). Substantiation Data for Hypersonic Cruise Vehicle Wing Structure Evaluation. Volume 1-3, NASA-CR-66897
9. Martinovic, Z. N. (2007). Structural Design and Analysis of Un-pressurized Cargo Delivery Vehicle. 48th AIAA/ASME/ASCE/AHS/ASC Structures, Structural Dynamics, and Materials Conference, Waikiki, USA
10. Martinovic, Z. N. (2009). Shuttle Orbiter-like Cargo Carrier on Crew Launch Vehicle. NASA-TM-2009-215793
11. Becker, M. (2013). Rettungskapsel Design und Integration für das Hyperschallverkehrsflugzeug SpaceLiner, Masterthesis, SART-TN-001/2014, DLR, Bremen
12. Kopp, A., Garbers, N. (2014). Investigation of Structure, Thermal Protection System, and Passenger Stage Integration for the Hypersonic Transport System SpaceLiner. 19th AIAA International Space Planes and Hypersonic Systems and Technologies Conference, Atlanta, USA – *to be published*